PROJECTILE SHAPE AND VELOCITY: IMPACT ON EJECTA DISTRIBUTION AND COMPOSITION; Noreen Joyce Evans and Thomas J. Ahrens, Lindhurst Laboratory of Experimental Geophysics, Seismological Laboratory, California Institute of Technology, Pasadena, CA 91125

Ejecta scaling using the results of hypervelocity impact recovery experiments is critical to advancing our understanding of natural impact phenomenon such as the theory of the giant impact melting of the early Earth and formation of the moon, the proposed impact degassing of Mercury, the origin of tektites on the Earth and the mechanisms associated with impact-related extinction. However, before ejecta scaling from experiments can be accomplished, the dependance of ejecta volume, distribution, grain-size and composition (projectile-target mixing) on impact parameters such as projectile shape and impact velocity must be determined. A series of hypervelocity impact experiments with different impact velocities and projectile geometries have been performed. We have found that the exact configuration of the projectile (e.g., the presence of a sabot which holds the metal sphere or disc) greatly affects ejecta distribution and projectile-target mixing.

A two-stage light gas gun was used to launch 6-7km/s projectiles into Mo targets (see Table). Ejecta fragments were captured by 0.032 g/cm^3 polystyrene foam (5cm thick) witness plates. After the impact, the witness plates were X-rayed and then sliced at regular longitudinal and transverse intervals to determine the depth of penetration and angular distribution of captured ejecta. Each section was dissolved in chloroform and the ejecta were recovered and weighed. Ejecta consisted of shards (unmelted) of target material (99% by mass) and melted ejecta which was composed of both target and projectile material, largely in spherical form. The spheres ($<$5-180 μm diameter) have distinct quench textures and were analyzed by electron microprobe to determine the proportions of target (Mo) and projectile (Fe) material in each (Figure 1). Sphere fragment velocities were determined by equating the energy expended during passage through the polystyrene foam to the kinetic energies of the fragments (1). For all shots, sphere velocity increases with increasing angle from the target surface. Velocities range from $<$5km/s to a maximum value of twice the impact velocity.

In shots where both the flyer and sabot impact the target (shots 1, 2 and 3) the maximum total ejecta mass is found in a jetted zone between 50-60°. Flyer shape, therefore, is not a control on the angular position of the jetted zone when a sabot is present.

The correlation of projectile-target mixing and ejection angle for shots 1 and 2 is distinctly different. In shot 1 the high angle, high velocity ejecta contains a higher projectile component than low angle, low velocity ejecta (Figure 1). In contrast, approximately equal proportions of target and projectile components are present in the melted ejecta of shot 2. The spheres recovered from shot 3 show highly variable projectile-target mixing but are relatively enriched in the projectile component. Projectile energy is also highest in this shot (see Table).

When the sabot is stripped and the flyer impacts the target alone (shot 4), X-rays of the witness plates indicate that the jetted zone occurs at a higher ejection angle (60-75°) and that virtually all of the ejecta is concentrated in this zone. Because the sabot adds considerable mass to the projectile (sabot is 7 times more massive than the flyer), the projectile mass and energy for shot 3 (sphere + sabot) were 8.5 times greater than those for shot 4. Accordingly, in shot 3, the crater volume was 6.3 times greater than in shot 4. The spherical flyer produced a crater with a more conical cross-section and a more prevalent raised rim than the projectile composed of a sphere plus sabot.

The measured crater volumes correlate well with crater volume scaling in the strength regime [(2), Figure 10] and provide experimental data for a higher ultimate strength target (Figure 2). The representation developed in (2) for 6-8km/s metal projectiles and metal targets fits the current data within inherent scatter, although the cratering efficiency for shot 4 is somewhat higher than for the

other shots (Figure 2).

These results indicate that, for cratering in the strength regime, when a sabot is present at impact, flyer shape exerts only minor control on the position of the jetted zone. Both projectile shape and impact velocity exert control projectile-target mixing. Whereas the disc + sabot impact at 6.6km/s led to an equal mixing of the projectile and target in the melted ejecta, the sphere + sabot impact at 6.9km/s produced spheres dominated by the projectile component. These shots fit well with crater volume scaling relationships developed in (2) and extend the previous data set to a higher strength regime. The energy partitioned to the impact by the sabot significantly effects crater morphology and ejecta distribution for high velocity experimental impacts in the strength regime. Since impact velocity and the presence of a sabot are critical controls on ejecta distribution and composition, ejecta scaling from experimental recovery experiments will only contribute to our understanding of terrestrial impact phenomenon if low strength targets and high velocity flyers without sabots are routinely used.

Shot	Flyer Composition	Projectile Shape	Impact Velocity (km/s)	Peak Shock Temperature and Pressure in Flyer	Projectile Energy ($J \times 10^3$)	Crater Volume (cm^3)
1	Fe-Ni-PGE[1] alloy	disc + sabot[2]	5.9	1740°C, 1.7Mb	7.9	0.78
2	Fe-Ni-PGE alloy	disc + sabot	6.6[3]	2944°C, 2.2Mb	9.9	0.92
3	stainless steel 302	sphere + sabot[4]	6.9	3088°C, 2.4Mb	11	0.95
4[5]	stainless steel 302	sphere	6.9	3088°C, 2.4Mb	1.3	0.15

[1]PGE = platinum-group elements (Ir, Ru, Pd, Pt) and Au. [3]The velocity for shot 2 was calculated from figure 10 in (2). [2]Disc inserted flush to impact face of sabot. [4]Sphere protrudes from impact face of the sabot by half its diameter (0.11 mm). [5]Weighing and microprobe analysis of the ejecta in shot 4 has yet to be performed. All targets were molybdenum.

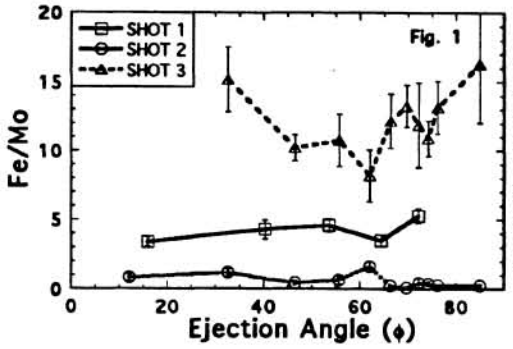

Figure 1. Mean Fe/Mo (mass ratio) versus angle of ejection (ϕ, angle from target surface). Error bars are standard deviation of the mean.

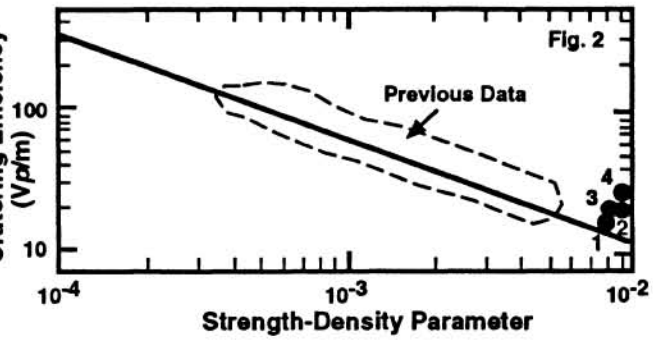

Figure 2. Crater volume scaling relationship (2) with present experimental data added.

(1) Evans, N.J., Ahrens, T.J., Shahinpoor, M. and Anderson, W.W. 1993. *Lunar Planet. Sci. Conf. XXIV*, March 15-19. (2) Holsapple, K.A. and Schmidt, R.M. 1982. J. Geophys. Res., **87**, 1849-1870.